Journal of Biomolecular NMR **82:** 185–190, 2004.
KLUWER/ESCOM

Triple resonance MAS NMR with (^{13}C, ^{15}N) labelled molecules: Reduced dimensionality data acquisition via ^{13}C-^{15}N heteronuclear two-spin coherence transfer pathways

Jörg Leppert, Bert Heise, Oliver Ohlenschläger, Matthias Görlach & Ramadurai Ramachandran*
Abteilung Molekulare Biophysik/NMR-Spektroskopie, Institut für Molekulare Biotechnologie, 07745 Jena, Germany

Received 23 June 2003; Accepted 3 September 2003

Key words: chemical shift correlation, magic angle spinning (MAS), reduced dimensionality experiments, solid-state NMR

Abstract

A reduced dimensionality magic angle spinning solid-state NMR experimental protocol for obtaining chemical shift correlation spectra of dipolar coupled nuclei in uniformly (^{13}C, ^{15}N) labelled biological systems is described and demonstrated. The method involves a mapping of the evolution frequencies of heteronuclear ^{13}C-^{15}N zero- and double-quantum coherences. In comparison to a reduced dimensionality procedure involving the simultaneous incrementation of two single-quantum chemical shift evolution periods, the approach described here could be potentially advantageous for minimising the heat dissipated in the probe by high power ^{1}H decoupling in experiments requiring long t_1 acquisition times.

Introduction

The introduction of techniques for inhibiting the spatial averaging of weak homo- and heteronuclear dipolar couplings between low γ nuclei has made possible the assignment of resonances and measurement of distances and torsion angles under magic angle spinning (MAS) (Bennett et al., 1994; Griffin, 1998; Dusold and Sebald, 2000; Baldus, 2002). This in turn has opened up exciting possibilities for the structural characterisation of biomolecules in the solid-state (Castellani et al., 2002; Rienstra et al., 2002), in particular of systems that are not easily amenable to solution state NMR investigations or X-ray crystallography (Jaroniec et al., 2002b; Petkova et al., 2002). As with solution state NMR, the pre-requisite for any MAS solid-state NMR-based structural study is the sequence specific assignment of resonances. To this end, a variety of RF irradiation schemes have been introduced in the literature for obtaining efficient multi-dimensional chemical shift correlation data in uniformly (^{13}C, ^{15}N) labelled peptides/proteins (Sun et al., 1997; Hong and Griffin, 1998; Hong, 1999; McDermott et al., 2000; Rienstra et al., 2000; Detken et al., 2001; Pauli et al., 2001; Astrof and Griffin, 2002; Petkova et al., 2003; Van Rossum et al., 2003). As improved spectral resolution is obtained with NMR data of higher dimensionality, typically an n-dimensional NMR experiment is carried out to correlate n different chemical shifts. For example, in the MAS SSNMR study of peptides/proteins, one can employ a 3D experiment involving the following magnetisation transfer pathways (Heise et al., 2002):

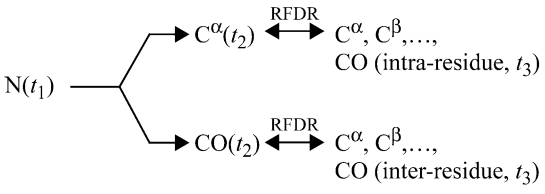

*To whom correspondence should be addressed. E-mail: raman@imb-jena.de

for making resonance assignments. Two amide nitrogens (and hence, amino acids) are identified as neighbours if the intra-residue ^{13}C (C^{α}, C^{β}, . . ., CO) chemical shifts of one of the nuclei is the same as the inter-residue ^{13}C (C^{α}, C^{β}, . . ., CO) chemical shifts of another. In the context of sequence specific resonance assignments, the $^{13}C \leftrightarrow {}^{13}C$ transfer step is a crucial element of the experimental protocol. Firstly, possible assignment ambiguities are minimised if two adjacent residues are linked at more than one ^{13}C position and secondly, a knowledge of the side chain carbon chemical shifts would also help in amino acid type identification. However, as each of the evolution periods of the indirect dimensions is sampled independently in a conventional multi-dimensional NMR experiment, increased spectral resolution in higher dimensional NMR data is obtained at the expense of increased data acquisition times. In this context, to minimise data acquisition time, Szyperski et al. (1993) and Simorre et al. (1994) have introduced in the solution state NMR literature the so called 'reduced dimensionality' (RD) experiments for correlating n chemical shifts in an NMR spectrum of dimensions less than n. For example, instead of the 3D experiment mentioned above, one can implement a 2D RD experiment in which the information about the chemical shifts of the ^{15}N and the carbon that is directly attached to the nitrogen is contained in the ω_1 dimension and the chemical shifts of all ^{13}C nuclei are contained in the ω_2 dimension. The utility of the RD experimental protocol is well documented (Brutscher et al., 1994, 1995a, b; Szyperski et al., 1998, 2002; Xia et al., 2002; Kim and Szyperski, 2003) and the RD approach has also been recently adapted to MAS solid-state NMR studies (Astrof et al., 2001; Luca and Baldus, 2002). The simplest version of the RD approach involves simultaneous frequency labelling of two different spins in a single indirect dimension of a multi-dimensional NMR experiment and this can be accomplished by two different methods.

In the first approach (as employed by, e.g., Astrof et al., 2001 and Kim and Szyperski, 2003), two single-quantum coherences of spins S_1 and S_2 are separately created at two different time intervals and are allowed to evolve with the same indirect dimension time variable t_1. The resultant signal detected in the acquisition dimension t_2 would be modulated by the two single-quantum evolution frequencies Ω_1 and Ω_2. If quadrature detection in the indirect dimension is effected on only one of the spins, say S_1, then the resultant spectrum in the ω_1 dimension would consist of a doublet centred at Ω_1 and separated by $2\Omega_2$. Considering uniformly labelled peptides, the RD correlation, for example, of the chemical shifts of the backbone ^{15}N and $^{13}C^{\alpha}/^{13}C'$ nuclei with those of the side chain carbons could involve a magnetisation transfer pathway of the type ^{15}N $(t_1) \rightarrow {}^{13}C^{\alpha}/^{13}C'$ $(t_1) \rightarrow {}^{13}C^{\beta}$, $^{13}C^{\gamma}$, . . . (t_2). The second approach to RD chemical shift correlation involves the creation of a two spin coherence of the type $S_{1x}S_{2x}$ and the mapping in a *single* time period t_1 the evolution frequencies of both the double and zero quantum coherences represented by the term $S_{1x}S_{2x}$ (Szyperski et al., 1993; Simorre et al., 1994). Considering once again the chemical shift correlation of the backbone ^{15}N and $^{13}C^{\alpha}/^{13}C'$ nuclei and the side chain carbons, an RD experiment based on the second approach would involve a magnetisation transfer pathway of the type $^{15}N_x{}^{13}C_x$ $(t_1) \rightarrow {}^{13}C^{\beta}$, $^{13}C^{\gamma}$, . . . (t_2). Both RD schemes could be equally effective in generating the desired chemical shift correlation data. However, in situations where long $(t_1)_{\max}$ acquisition times are needed for improved spectral resolution, the second approach involving only a single t_1 evolution period may be preferable for minimising the heat dissipated by high power ^1H decoupling typically employed in solid-state NMR studies. Hence, an RF pulse scheme based on the second RD approach will be highly valuable in MAS NMR structural studies of uniformly labelled peptides/proteins and it has been recently implemented (Figure 1) in our laboratory. The details of the RF pulse sequence are given below.

After cross polarisation from ^1H, the RF pulse scheme shown in Figure 1 employs the REDOR procedure, as in the 2D N(CO)CA and 3D N(CA)CB sequences of Hong (1999), for the conversion of the single-quantum coherence $^{13}C_y$ to the anti-phase operator term $^{13}C_x{}^{15}N_z$. The phases of the 90° RF pulses applied to the carbon and nitrogen spins at the end of the REDOR mixing period are chosen such that the anti-phase operator term is converted to the heteronuclear two spin coherence $^{15}N_x{}^{13}C_x$ and allowed to evolve in t_1. At the end of the t_1 evolution period, the $^{15}N_x{}^{13}C_x$ term is converted back to the single-quantum coherence $^{13}C_x{}^{15}N_z$ and subsequently refocussed by the second REDOR sandwich to the $^{13}C_y$ term. Broadband RFDR with adiabatic inversion pulses (Heise et al., 2002; Leppert et al., 2003) is then employed for effecting longitudinal magnetisation transfer from ^{15}N-connected ^{13}C spins to other ^{13}C nuclei. A short RFDR mixing time ensures that the magnetisation transfer takes place only among ^{13}C nuclei in spatial proximity (e.g., one-bond distance).

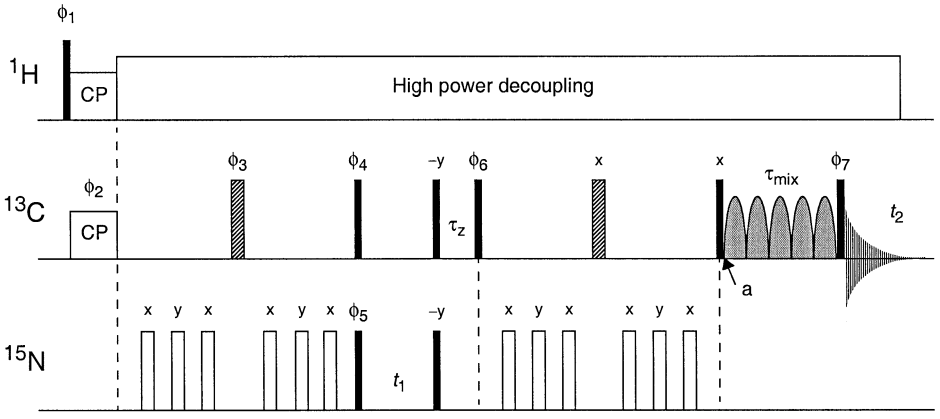

Figure 1. RF pulse sequence for reduced dimensionality chemical shift correlation in uniformly labelled peptides or proteins under magic angle spinning. Open and filled rectangles represent 180° and 90° pulses, respectively. Hatched rectangles indicate refocussing pulses that can be either broadband or band selective. RFDR with adiabatic inversion pulses is employed to induce polarisation transfer from ^{15}N attached ^{13}C nuclei to other carbons. For RFDR mixing, the ^{13}C carrier is switched at point *a* from the value employed during t_1 to the middle of the ^{13}C spectral range. Phase cycling employed: $\phi_1 = (y, -y)$; $\phi_2 = -y$; $\phi_3 = \phi_4 = x$; $\phi_5 = (y, y, -y, -y)$; $\phi_6 = (4(y), 4(-y))$; $\phi_7 = (8(x), 8(y), 8(-x), 8(-y))$; $\phi_{rec} = (-x, x, x, -x, x, -x, -x, x), (-y, y, y, -y, y, -y, -y, y), (x, -x, -x, x, -x, x, x, -x), (y, -y, -y, y, -y, y, y, -y)$. Phase sensitive 2D spectra with ω_1 quadrature detection only in ^{15}N is obtained by incrementing the phase ϕ_5 while for quadrature detection in both the heteronuclei, 4 data sets were collected by independently incrementing the phases ϕ_5 and (ϕ_2, ϕ_3, ϕ_4), as per States et al. (1982).

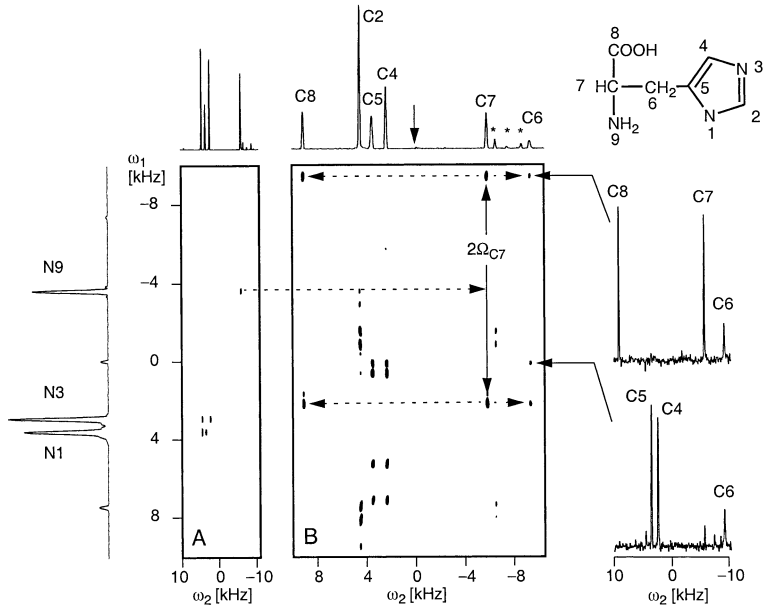

Figure 2. Conventional one-bond (A) and RD dimensionality (B) 2D ^{15}N-^{13}C heteronuclear chemical shift correlation spectra of histidine. The RD spectrum (zoomed plot) was collected employing a spinning speed of 11 kHz, 128 t_1 increments, 44 kHz spectral width in ω_1, 32 scans per t_1 increment, 2 s recycle time, RFDR mixing time of 1.82 ms and with ω_1 quadrature detection only on ^{15}N. Resonance assignments given in the spectral projections are as per Sun et al. (1997). The ^{13}C carrier position employed in the t_1 dimension of the RD spectrum is indicated by an arrow in the ^{13}C spectral projection (top). Peaks marked with an asterisk are spinning sidebands. RFDR mixing is achieved employing a (0°, 240°, 240°, 60°, 0°) phase cycle (Tycko et al., 1985; Leppert et al., 2003) with cagauss adiabatic inversion pulses (Kupce and Freeman, 1996; Leppert et al., 2002, 2003) of 91 μs duration (42 kHz γ H_1) and having a sweep width of 80 kHz. Spectral cross sections shown were taken at the positions indicated in the RD spectrum.

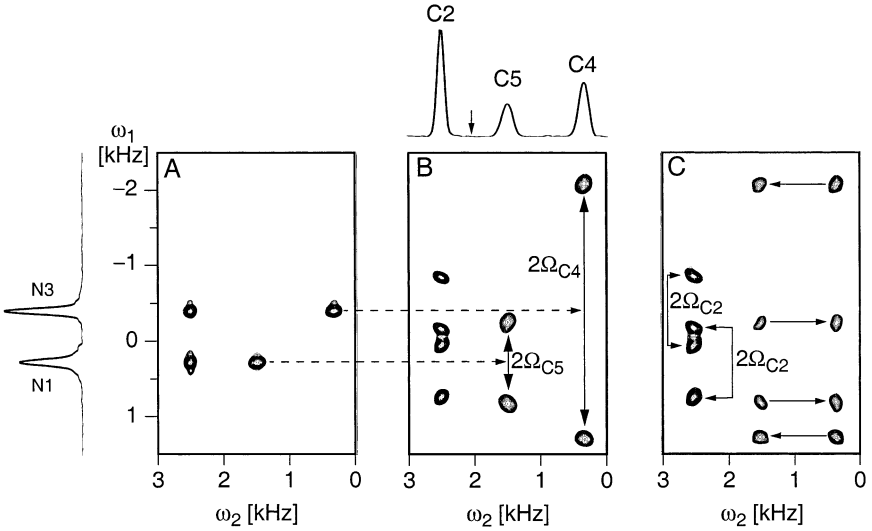

Figure 3. RD ^{15}N-^{13}C correlation spectra (aromatic region) of histidine without (B) and with (C) RFDR mixing. For comparison, the conventional one-bond heteronuclear spectrum is given in Figure 3A. The ^{13}C carrier position employed in the t_1 dimension is indicated in the projected ^{13}C RD spectrum (arrow). The RD spectrum (zoomed plot) was collected employing a spectral width of 11 kHz in ω_1 and an RFDR mixing time of 1.36 ms. All other parameters employed were as in Figure 2.

Following the t_1 evolution period, the spin system is kept in the $^{15}N_z{}^{13}C_z$ state for a short duration τ_z. This ensures that the total delay between the REDOR mixing periods equals an integral number of rotor cycles and thereby achieves efficient reconversion of the antiphase coherence $^{13}C_x{}^{15}N_z$ to the in-phase term $^{13}C_y$ (Hong and Griffin, 1998; Jaroniec et al., 2002a). At the end of the t_1 period additional coherences of the type $^{15}N_x{}^{13}C_y$, etc. would also be present (Simorre et al., 1994). To obtain 2D cross peaks without any phase distortion (Simorre et al., 1994) the phases of the 90° RF pulses applied to the carbon and nitrogen spins at the end of the t_1 evolution period are chosen such that only the $^{15}N_x{}^{13}C_x$ is converted back to a ^{13}C single-quantum coherence and that the contributions to the observed signal from the other terms are eliminated. As the two spin coherence $^{15}N_x{}^{13}C_x$ is essentially a combination of heteronuclear zero- and double-quantum coherences ($I_N^+ I_C^-$, $I_N^+ I_C^+$, etc.), the evolution of this coherence in t_1 would result in a modulation of the signal detected in the acquisition dimension by the zero- and double-quantum frequencies ($\Omega_N - \Omega_C$) and ($\Omega_N + \Omega_C$), respectively. If quadrature detection in the indirect dimension is effected only on one of the spins, say ^{15}N, then the resultant spectrum in the ω_1 dimension would consist of a doublet centred at Ω_N and separated by $2\Omega_C$. We have assessed the efficacy of the RD approach presented here by acquiring 2D spectral data from a uniformly ^{13}C and ^{15}N labelled undiluted sample of histidine that has been employed as a model system in several recent MAS NMR investigations (Michal and Jelinski, 1997; Sun et al., 1997). The spectra were collected at room temperature employing a wide bore 500 MHz Varian $^{\text{UNITY}}$*INOVA* solid-state NMR spectrometer equipped with a 5 mm DOTY supersonic triple resonance probe and waveform generators for pulse shaping. Other relevant details are given in the figure captions.

Figures 2A and 2B show a conventional MAS 2D ^{15}N-^{13}C heteronuclear correlation spectrum of histidine recorded at a spinning speed of 11 kHz and a corresponding RD spectrum obtained employing an RFDR mixing time of 1.82 ms. Resonance assignments are indicated in the spectral projections and a few representative cross-sections are also given. The RD spectrum was collected by keeping the ^{13}C carrier approximately at the centre of the spectral range in both the dimensions. In view of the short REDOR mixing times employed, the ^{15}N-^{13}C RD correlation spectrum shows, as in Figure 2A, only cross peaks arising from short range (one-bond) heteronuclear dipolar interactions. Cross peaks in the RD spectrum appear as doublets in the ω_1 dimension with the separation between the doublets corresponding to twice the offset of the ^{13}C resonances from the ^{13}C carrier frequency. Each of the ω_1 spectral doublets is centred at the corresponding ^{15}N chemical shift position seen in the conventional ^{15}N-^{13}C correlation spectrum (Fig-

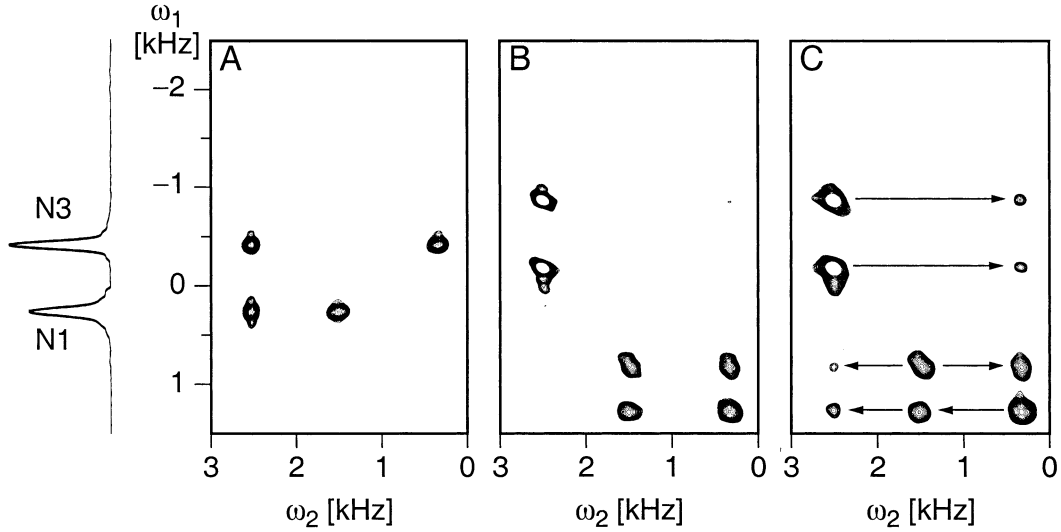

Figure 4. Zero-quantum RD ^{15}N-^{13}C correlation sub-spectra (aromatic region) of histidine obtained with RFDR mixing times of 1.36 ms (B) and 3.2 ms (C). For comparison, the conventional one-bond heteronuclear spectrum is also given in Figure 4A. Four data sets were collected by independently incrementing the phases ϕ_5 and (ϕ_2 ϕ_3, ϕ_4) according to the States procedure. Other parameters employed were as in Figure 3.

ure 2A). Besides the direct correlation peaks, additional cross peaks arising from RFDR mixing are also seen in the RD spectrum. For the ^{15}N9-^{13}C7-^{13}C8 spin network, as an example, all relevant features have been indicated in Figure 2B. The spectral cross sections shown in Figure 2 clearly show peaks arising from ^{13}C7 $\rightarrow$ ^{13}C6 and ^{13}C4 $\rightarrow$ ^{13}C5 $\rightarrow$ ^{13}C6 polarisation transfers. In the RD spectrum given in Figure 2B, only direct correlation peaks arising from ^{15}N1,3 $\leftrightarrow$ ^{13}C2 heteronuclear dipolar interactions are seen. However, as will be shown below, employing longer RFDR mixing times it is also possible to link the ^{13}C2 resonance to the aromatic spin network of histidine. The correlation patterns seen in Figure 2B are consistent with the previously reported 3D ^{15}N-^{13}C-^{13}C data of histidine (Sun et al., 1997).

It is worth noting that the ^{13}C carrier position in the ω_1 dimension may be such that some of the cross peaks in the RD spectrum may accidentally overlap or unambiguous identification of symmetry related peaks may become difficult. To reduce ambiguities in resonance assignments, it may be necessary to collect the RD spectrum with more than one ^{13}C carrier frequency position in the ω_1 dimension. Collection of such RD data would result in spectra in which the separation between the ω_1 doublets vary without any changes in their mean position. As an example, we show in Figure 3 RD spectral data collected employing a different ^{13}C carrier position compared to what was used in Figure 2B. To provide better visual clarity, only the aromatic region of the spectrum is shown. Figure 3A shows the normal heteronuclear correlation spectrum and Figures 3B and 3C show RD spectra collected employing RFDR mixing times of zero and 1.35 ms, respectively. The effect of ^{13}C carrier position in ω_1 and the efficiency of magnetisation transfer from the ^{15}N attached ^{13}C spin to other carbons can be clearly seen. The RD spectra shown in Figures 2 and 3 were obtained by applying ω_1 quadrature detection only on the ^{15}N nucleus. Hence, from the frequency separation of the ω_1 doublets it is not possible to obtain the sign of the ^{13}C resonance offset. This difficulty can be overcome either by keeping the ^{13}C carrier frequency at one end of the spectral range or by applying ω_1 quadrature detection to both the ^{15}N and ^{13}C nuclei. The latter option would not only permit the positioning of the ^{15}N and ^{13}C carrier frequencies at the centre of the spectral range but also minimise spectral overlaps by allowing the decomposition of the RD spectrum into two separate sub-spectra containing either heteronuclear zero- ($\Omega_N - \Omega_C$) or double-quantum ($\Omega_N + \Omega_C$) cross peaks. With the RF pulse sequence given in Figure 1 it is possible to apply ω_1 quadrature detection to both the heteronuclei by *independently* incrementing the phases ϕ_5 and (ϕ_2, ϕ_3, ϕ_4) according to States procedure (States et al., 1982). Complex Fourier transformation of appropriate linear combinations of the resulting four quadrature components (I) $\cos(\omega_N t_1)$ $\cos(\omega_C t_1)$, (II) $\cos(\omega_N t_1)$ $\sin(\omega_C t_1)$, (III) $\sin(\omega_N t_1)$ $\cos(\omega_C t_1)$ and (IV) $\sin(\omega_N$

t_1) sin(ω_C t_1) would then yield the desired zero- and double-quantum RD spectra (Brutscher et al., 1995b). As an example, we show in Figure 4 the zero-quantum RD sub-spectra of the aromatic region collected at two different RFDR mixing times. These spectra were collected by keeping the ^{13}C RF carrier in t_1 at the same position as in Figure 3. The spectrum obtained with an RFDR mixing time of 3.2 ms (Figure 4C) clearly shows cross peaks arising from C2 $\leftrightarrow$ C4 magnetisation transfer and enables the linking of the C2 resonance to the aromatic spin network of histidine.

In conclusion, from the RD spectral data presented here, it is clearly seen that the RF pulse sequence given in Figure 1 can be effectively employed for obtaining chemical shift correlation data involving the ^{15}N and ^{13}C backbone and side chain resonances of uniformly labelled peptides and proteins. Considering the peptide backbone, the intra- and inter-residue correlations and hence the sequential resonance assignments can be obtained either in a single or two different experiments depending on whether the 180° refocussing pulses employed achieve broadband or band selective excitation. A pre-requisite for the successful application of the RD approach in sequential resonance assignments studies is that the ^{15}N-^{13}C cross peaks in a conventional heteronuclear correlation spectrum should not overlap in at least one of the dimensions. At high magnetic field strengths it is conceivable that RD experiments can be successfully employed in the study of medium sized molecules or large proteins with (segment) specific labelling. Astrof et al. (2001) recently presented RD MAS NMR sequences based on simultaneous incrementation of two single-quantum evolution periods. The RD approach outlined here is complementary to their study and could be useful in experiments with long $(t_1)_{max}$.

References

Astrof, N.S. and Griffin, R.G. (2002) *J. Magn. Reson.*, **158**, 157–163.

Astrof, N.S., Lyon, C.E. and Griffin, R.G. (2001) *J. Magn. Reson.*, **152**, 303–307.

Baldus, M. (2002) *Prog. NMR Spectrosc.*, **41**, 1–47.

Bennett, A.E., Griffin, R.G. and Vega, S. (1994) In *NMR Basic Principles and Progress*, Vol. 33, Blümich, B. and Kosfeld, P. (Eds.), Springer-Verlag, Berlin, pp. 1–77.

Brutscher, B., Cordier, F., Simorre, J.P., Caffrey, M.S. and Marion, D. (1995a) *J. Biomol. NMR*, **5**, 202–206.

Brutscher, B., Morelle, N., Cordier, F. and Marion, D. (1995b) *J. Magn. Reson.*, **B109**, 238–242.

Brutscher, B., Simorre, J.P., Caffrey, M.S. and Marion, D. (1994) *J. Magn. Reson.*, **B105**, 77–82.

Castellani, F., van Rossum, B., Diehl, A., Schubert, M., Rehbein, K. and Oschkinat, H. (2002) *Nature*, **420**, 98–102.

Detken, A., Hardy, E.H., Ernst, M., Kainosho, M., Kawakami, T., Aimoto, S. and Meier, B.H. (2001) *J. Biomol. NMR*, **20**, 203–221.

Dusold, S. and Sebald, A. (2000) *Annu. Rep. NMR Spectrosc.*, **41**, 185–264.

Griffin, R. (1998) *Nat. Struct. Biol.*, **5**, 508–512.

Heise, B., Leppert, J., Ohlenschläger, O., Görlach, M. and Ramachandran, R. (2002) *J. Biomol. NMR*, **24**, 237–243.

Hong, M. (1999) *J. Biomol. NMR*, **15**, 1–14.

Hong, M. and Griffin, R.G. (1998) *J. Am. Chem. Soc.*, **120**, 7113–7114.

Jaroniec, C.P., Filip, C. and Griffin, R.G. (2002a) *J. Am. Chem. Soc.*, **124**, 10728–10742.

Jaroniec, C.P., MacPhee, C.E., Astrof, N.S., Dobson, C.M. and Griffin, R.G. (2002b) *Proc. Natl. Acad. Sci. USA*, **99**, 16748–16753.

Kim, S. and Szyperski, T. (2003) *J. Am. Chem. Soc.*, **125**, 1385–1393.

Kupce, E. and Freeman, R. (1996) *J. Magn. Reson.*, **A118**, 299–303.

Leppert, J., Heise, B., Görlach, M. and Ramachandran, R. (2002) *J. Biomol. NMR*, **23**, 227–238.

Leppert, J., Heise, B., Ohlenschläger, O., Görlach, M. and Ramachandran, R. (2003) *J. Biomol. NMR*, **26**, 13–24.

Luca, S. and Baldus, M. (2002) *J. Magn. Reson.*, **159**, 243–249.

McDermott, A., Polenova, T., Böckmann, A., Zilm, K.W., Paulson, E.K., Martin, R.W., Montelione, G.T. and Paulsen, E.K. (2000) *J. Biomol. NMR*, **16**, 209–219.

Michal, C.A. and Jelinski, L.W. (1997) *J. Am. Chem. Soc.*, **119**, 9059–9060.

Pauli, J., Baldus, M., van Rossum, B., de Groot, H. and Oschkinat, H. (2001) *Chembiochem*, **2**, 272–281.

Petkova, A.T., Baldus, M., Belenky, M., Hong, M., Griffin, R.G. and Herzfeld, J. (2003) *J. Magn. Reson.*, **160**, 1–12.

Petkova, A.T., Ishii, Y., Balbach, J.J., Antzutkin, O.N., Leapman, R.D., Delaglio, F. and Tycko, R. (2002) *Proc. Natl. Acad. Sci. USA*, **99**, 16742–16747.

Rienstra, C.M., Hohwy, M., Hong, M. and Griffin, R.G. (2000) *J. Am. Chem. Soc.*, **122**, 10979–10990.

Rienstra, C.M., Tucker-Kellogg, L., Jaroniec, C.P., Hohwy, M., Reif, B., McMahon, M.T., Tidor, B., Lozano-Perez, T. and Griffin, R.G. (2002) *Proc. Natl. Acad. Sci. USA*, **99**, 10260–10265.

Simorre, J., Brutscher, B., Caffrey, M.S. and Marion, D. (1994) *J. Biomol. NMR*, **4**, 325–333.

States, D.J., Haberkorn, R.A. and Ruben, D.J. (1982) *J. Magn. Reson.*, **48**, 286–292.

Sun, B.-Q., Rienstra, C.M., Costa, P.R., Williamson, J.R. and Griffin, R.G. (1997) *J. Am. Chem. Soc.*, **119**, 8540–8546.

Szyperski, T., Banecki, B., Braun, D. and Glaser, R.W. (1998) *J. Biomol. NMR*, **11**, 387–405.

Szyperski, T., Wider, G., Bushweller, J.H. and Wüthrich, K. (1993) *J. Biomol. NMR*, **3**, 127–132.

Szyperski, T., Yeh, D.C., Sukumaran, D.K., Moseley, H.N. and Montelione, G.T. (2002) *Proc. Natl. Acad. Sci. USA*, **99**, 8009–8014.

Tycko, R., Pines, A. and Guckenheimer, J. (1985) *J. Chem. Phys.*, **83**, 2775–2802.

Van Rossum, B.J., Castellani, F., Pauli, J., Rehbein, K., Hollander, J., De Groot, H.J. and Oschkinat, H. (2003) *J. Biomol. NMR*, **25**, 217–223.

Xia, Y., Arrowsmith, C.H. and Szyperski, T. (2002) *J. Biomol. NMR*, **24**, 41–50.